Optimized Junction Termination Extension and Ring System for 11 kV 4H-SiC BJT

Ali Ammar, Mihai Lazar, Bertrand Vergne, Sigo Scharnholz, Luong Viêt Phung, Camille Sonneville, Christophe Raynaud, Hervé Morel, Dominique Planson, Marcin Zielinski

Optimized Junction Termination Extension and Ring System for 11 kV 4H-SiC BJT

Ali Ammar*, Mihai Lazar, Bertrand Vergne***, Sigo Scharnholz***, Luong Phung Viet*, Camille Sonneville*, Christophe Raynaud*, Herve Morel*, Dominique Planson*, Marcin Zielinski**

*Univ Lyon, INSA Lyon, Université Claude Bernard Lyon 1, Ecole Centrale de Lyon, CNRS, AMPERE, F-69621, Lyon, France.
**Université de Technologie de Troyes, 10300, Troyes, France
***Institut Recherches Franco-Allemand de Saint Louis, 68300, Saint Louis, France

ali.ammar@insa-lyon.fr,mihai.lazar@utt.fr,bertrand.vergne@isl.eu, sigo.scharnholz@isl.eu,luong-viet.phung@insa-lyon.fr,dominique.planson@insa-lyon.fr,herve.morel@insa-lyon.fr,camille.sonneville@insa-lyon.fr, mzielinski@novasic.com

Abstract*: In this article, a high power 4H-SiC NPN BJT is demonstrated with a blocking voltage greater than 10 kV when its theoretical value is around 13 kV. The device design was extracted from a previous reported model and eleven fabrication process were performed. The maximum common-emitter current gain recorded is 20 at 178 A/cm².

Keywords: Bipolar Devices, 4H-SiC BJT, blocking voltage, I-V characteristics, TCAD modeling.

1. Introduction

High voltage bipolar devices such as BJTs based on 4H-SiC are considered a very attractive candidate for high power applications. In particular, when compared to silicon thanks to a high breakdown electric field resulting in decreasing the ON resistance and probably avoiding a second breakdown avalanche effect [1]. In addition, a high saturation velocity enables fast switching and a wide band gap allows it to operate over high temperatures [2]. Finally, a good thermal conductivity giving it the ability to easily transfer the heat generated by Joule's effect to a heat sink [3]. The recent literature reported high voltage 4H-SiC BJTs include a 10-kV open-base breakdown voltage (BV_{CEO}) and a specific on-resistance of 130 mΩ.cm2 at (RT) with a 120 µm drift layer doped to $6x10^{14}$ cm^{-3} [4]. A 15 kV (BV_{CEO}) at a leakage current of 0.1 mA/cm^2 with 125 µm drift layer doped to 1.1 $x10^{14}$ cm^{-3} [5]. And a 9.2 kV (BV_{CEO}) with a 50 µm, 7 $x10^{14}$ cm^{-3} doped drift layer and R_{SP_ON} = 78 mΩ.cm^2 [6]. For high voltage applications, it is mandatory to implant a highly sophisticated base-drift junction termination extension (JTE), which serves in minimizing the electric field plate crowd generated at the MESA edge of the power device. Several approaches were applied to optimize the extension performance such that applying variations over the length and etching depth of the JTE [7], or by implanting different doses over the total length of the JTE [8], and by the addition of extra implanted rings [9]. In this paper a ≥ 10 kV NPN BJT based on 4H-SiC is reported when the theoretical value determined by its drift layer thickness and doping concentration is almost 13 kV.

2. Device Design and Fabrication

Fig. 1-a) represents a cross-sectional view of a fabricated BJT with five epitaxial layers grown in one continuous run on a ~300 µm 4° off-axis 4H-SiC substrate. Eleven photo-lithographic levels have been processed during the fabrication of the NPN BJT. The first two concern the 0.5 µm plasma etching of the n-type emitter doped to $1x10^{19}$ cm^{-3} meeting another 0.5 µm emitter highly doped to $3x10^{19}$ cm^{-3}, and a 2 µm p-type base doped to $2x10^{17}$ cm^{-3} in SF_6 chemistry with an ICP/RIE (Inductively Coupled Plasma-Reactive Ion Etching) Plassys MU400 reactor. The process has been optimized with high ICP density plasma (1000W) and high applied RIE bias (~350V) to obtain quasi-vertical trenches with rounded sides at the bottom part (Fig. 2) to avoid equipotential line tightening and high electric field peaks in this area, under reverse bias at high voltage. After plasma etching two doping steps with Al ion implantations have been performed, under the p-type base to ensure a low resistive ohmic contact and to implant

the peripheral protection. To avoid SiC amorphization the high doped base wells have been implanted at 300°C. To activate

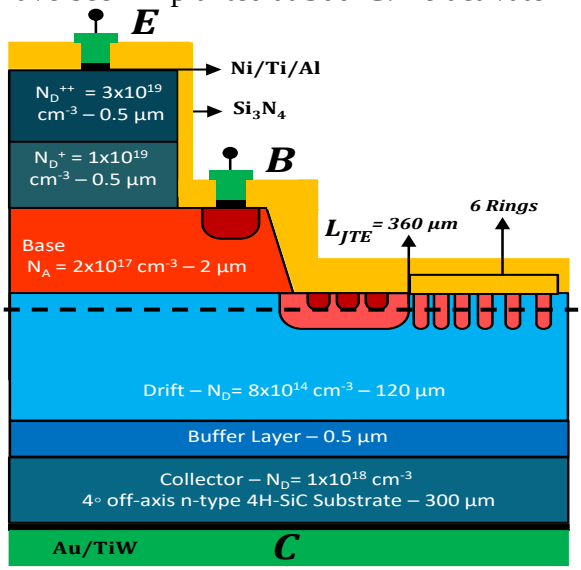

(a)

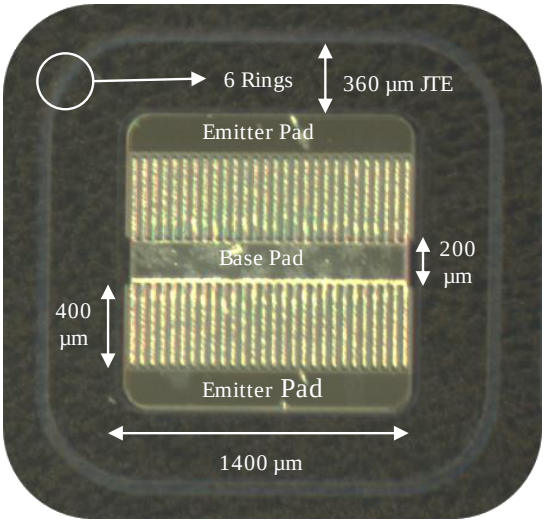

(b)

Fig. 1: Schematic cross-sectional view of 4H-SiC NPN BJT (a). Top microscopic view of 0.053 cm^2 fabricated device with 2 emitter pads (b).

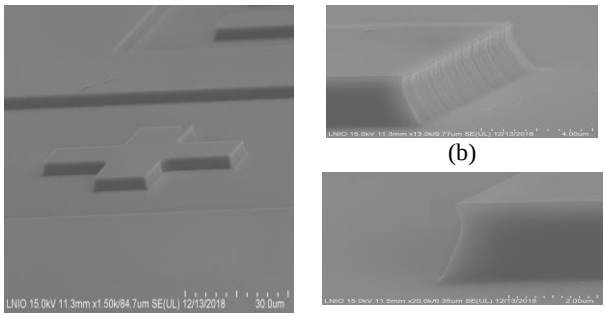

(a) (c)

Fig. 2: Quasi-vertical trenches with rounded sides at the bottom part.

dopants, post-implantation annealing has been performed with a 1700°C/30 min plateau in an AET 6' RTP furnace with graphite resistors, specially designed for this process (Fig. 3). Previously the samples have been encapsulated on the both sides with a C-cap obtained by pyrolyzing AZ photoresist. The C-cap has been after removed by O_2 plasma. The lowly n-doped drift layer has a thickness of 120 µm and a doping concentration 8x10^{14} cm^{-3}.

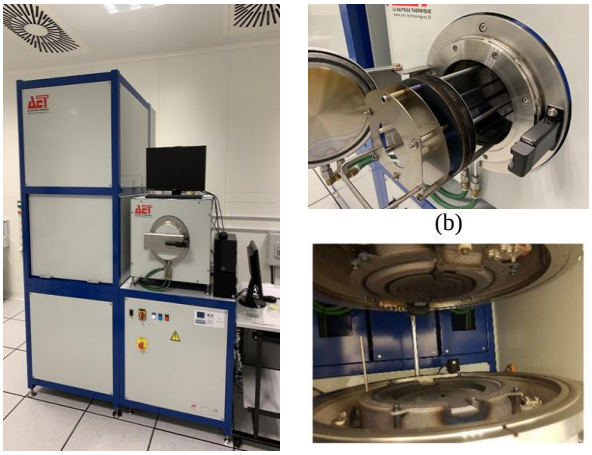

(a) (b) (c)

Fig. 3 AET furnace with RTP (c) and pyrolyze (b) chambers

The next technological steps have concerned the metallization with ohmic contacts formed on the high p-doped and n-doped (both sides) layers. For the n-type emitter and collector, sputtering Ni layers were patterned, and RTA annealed at 900°C and an alloy of Ni/Ti/Al 800°C RTA annealed [10] for the p-type base contacts. For making uniform potential distribution along metallized fingers, gold over-metallization

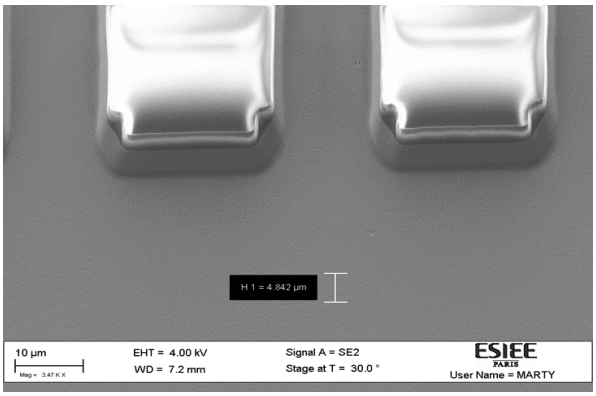

Fig. 4: An image during the technological process with the BJT defined fingers

has been also performed by sputtering and patterned. Before the metallization steps, SiC wafers have been thermal oxidized with a combined wet/dry process and the different metallic layers were isolated with LPCVD and PECVD Si_3N_4 layers locally opened by SF_6 plasma RIE. At the end a last passivation layer has been patterned in surface with a thick polyimide of 12 µm.

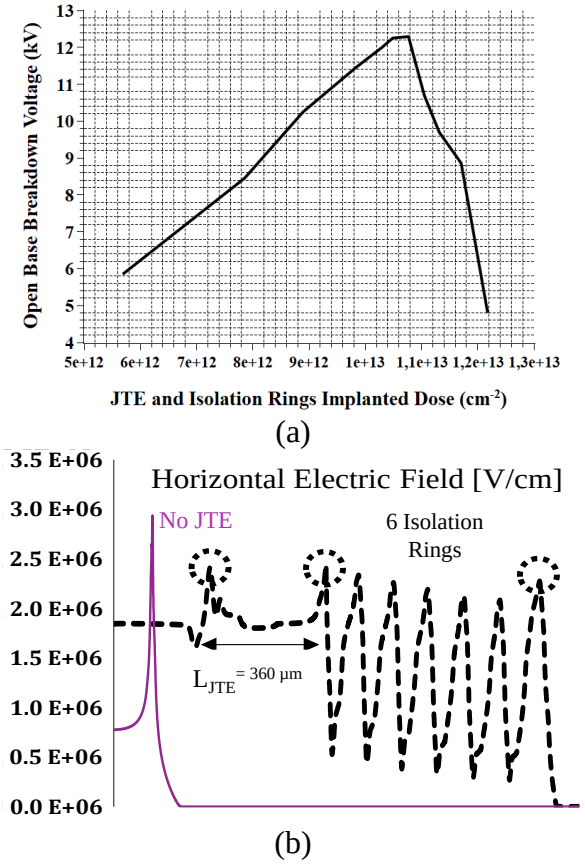

Fig. 5: Variation of Blocking Voltage (kV) as a function of JTE implanted Dose in cm^{-2} (a). Electric field distribution over the horizontal axis through the peripheral protection – Cross Section is shown in Fig. 1-a) "Dashed Line" (b).

The peripheral protection is made up of 360 µm JTE done by Al implantation with an optimum dose of 1.1x13 cm^{-2} (Fig. 5-a). Additional 6 rings are added each of a 5 µm length with a 4-um space between the JTE and first ring. The peripheral protection design and parameters such as JTE length, rings number, and implanted dose were extracted from [11] upon a study done on a simulation model using TCAD from Synopsyes Sentaurus [12] by performing various breakdown simulations to detect optimum technological parameters. The electric field distribution shown in (Fig. 5-b) describes the impact of having such an optimized system to ensure a smooth flow of the high electric field crowd that gathers at the junction termination through all the device, increasing by this phenomenon the blocking voltage.

3. Results and Discussion

Electrical characterizations were performed on the fabricated devices. Reverse IV-characteristics as shown in Fig. 6 were performed using the testbench in Franco-German Institute of Saint Louis [13]. A high blocking voltage of 11 kV with 0.1 mA/cm^2 leakage current density was recorded validating our model and simulation results. The efficiency of our peripheral protection can be now clearly visualized when comparing both graphs in (Fig. 5 -b) and Fig. 6. The distribution of the electric field all over the device due to the junction termination extension (black curve) when compared to the electric field in the absence of a JTE (purple curve) lead to a great increase in blocking voltage from 1.3 kV when JTE absent and 11 kV with a JTE.

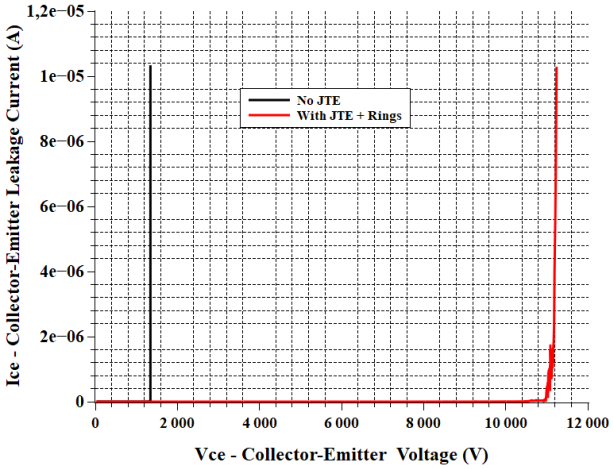

Fig. 6: Reverse IV Characteristics recording an open emitter blocking voltage of 11 kV at room temperature. The recorded results belong to the device shown in Fig. 1-b).

Fig. 7 shows forward common-emitter *I-V* characteristics and a Gummel plot at room temperature, of the fabricated BJT (Fig. 1-b) with an active area of 0.56 mm^2 when emitter finger width is 20 µm. The maximum current gain achieved is (β = 20) at a base

current (I_B = 50 mA) and V_{CE} = 13 V for a collector current I_C = 1A (Cyan Curve) giving a current density of 178 A/cm^2.

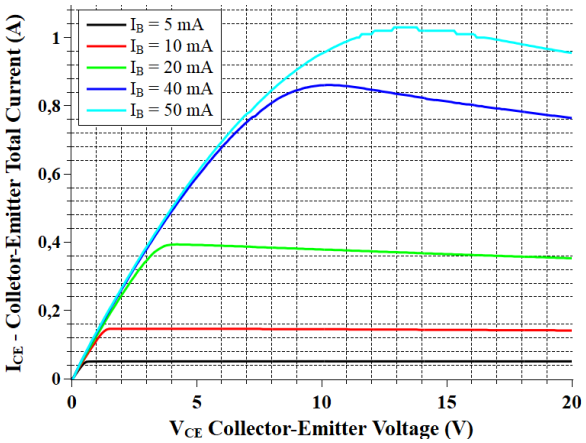

Fig. 7: Forward *I-V* characteristics of fabricated BJT with an active area of 0.0056 cm^2.

4. Summary

In this article, a 10+ kV class BJT based on 4H-SiC is reported with a well-studied junction termination extension and isolation ring system. The fabricated device attained an 11 kV as open base blocking voltage which corresponds almost to 90% of its theoretical value, at a 10 µA leakage current. The device also shows at room temperature a maximum current gain (β = 20) at base current 50 mA and current density 178 A/cm^2 and a total collector current of 1 A. The next target will be to characterized optical controlled BJT designed in the project.

Acknowledgment This study was supported by a grant overseen by the French National Research Agency (ANR), the project HV-Photo-Switch, ANR-18-CE05-0020-01. The experiments were carried out within the ESIEE (www.esiee.fr/en/about-esiee/cleanrooms) and Nanomat platforms (www.nanomat.eu).

References

[1] J. A. Cooper and A. Agarwal, "SiC power-switching devices-the second electronics revolution?," *Proc. IEEE*, vol. 90, pp. 956–968, 2002.

[2] M. Locatelli, "Silicon carbide against silicon: a comparison in terms of physical properties, technology and electrical performance of power devices," *J. Phys. III, EDP Sci.*, vol. 1, pp. 1101–1110, 1993.

[3] S. Krishnaswami *et al.*, "1000-V, 30-A 4H-SiC BJTs with high current gain," *IEEE Electron Device Lett.*, vol. 26, no. 3, pp. 175–177, 2005, doi: 10.1109/LED.2004.842731.

[4] Q. Zhang *et al.*, "10 kV, 10 A bipolar junction transistors and darlington transistors on 4H-SiC," *Mater. Sci. Forum*, vol. 645–648, pp. 1025–1028, 2010, doi: 10.4028/www.scientific.net/MSF.645-648.1025.

[5] A. Salemi, H. Elahipanah, K. Jacobs, C. M. Zetterling, and M. Östling, "15 kV-Class Implantation-Free 4H-SiC BJTs with Record High Current Gain," *IEEE Electron Device Lett.*, vol. 39, no. 1, pp. 63–66, 2018, doi: 10.1109/LED.2017.2774139.

[6] E. G. Turitsyna and S. Webb, "Simple design of FBG-based VSB filters for ultra-dense WDM transmission ELECTRONICS LETTERS 20th January 2005," *Electron. Lett.*, vol. 41, no. 2, pp. 40–41, 2005, doi: 10.1049/el.

[7] A. Salemi, H. Elahipanah, G. Malm, C. M. Zetterling, and M. Ostling, "Area- and efficiency-optimized junction termination for a 5.6 kV SiC BJT process with low ON-resistance," *Proc. Int. Symp. Power Semicond. Devices ICs*, vol. 2015-June, pp. 249–252, 2015, doi: 10.1109/ISPSD.2015.7123436.

[8] H. Miyake, T. Okuda, H. Niwa, T. Kimoto, and J. Suda, "21-kV SiC BJTs with space-modulated junction termination extension," *IEEE Electron Device Lett.*, vol. 33, no. 11, pp. 1598–1600, 2012, doi: 10.1109/LED.2012.2215004.

[9] D. M. Nguyen *et al.*, "Edge termination design improvements for 10 kV 4H-SiC bipolar diodes," *Mater. Sci. Forum*, vol. 740–742, pp. 609–612, 2013, doi: 10.4028/www.scientific.net/MSF.740-742.609.

[10] F. Laariedh, M. Lazar, P. Cremillieu, J. Penuelas, J. L. Leclercq, and D. Planson, "The role of nickel and titanium in the formation of ohmic contacts on p-type 4H-SiC," *Semicond. Sci. Technol.*, vol. 28, no. 4, 2013, doi: 10.1088/0268-1242/28/4/045007.

[11] A. Ammar, L. V. Phung, D. Planson, H. Morel, and C. Sonneville, "Design and Methodology of Silicon Carbide High Voltage Termination Extension for Small Area BJTs," *Mater. Sci. Forum*, vol. 1062, pp. 613–618, 2022, doi: 10.4028/p-vms03o.

[12] "Sentaurus TCAD Simulation Tool by Synopsys Inc." 2019.

[13] B. Vergne, S. Scharnholz, R. Hassdorf, D. Planson, D. Tournier, and P. Brosselard, "Recise Automated Semiconductor Characterization Under Ambient Control (Paschac) – an Advanced Test Bench for High-Voltage Semiconductor Devices," pp. 23–28, 2015.